Development and Enhancement of a Four-Port MIMO Antenna Optimized for 5G with Increased Isolation

Linda Chouikhi[1,*], Chaker Essid[1] and Bassem Ben Salah[1]

[1]SERCOM Laboratory, Tunisia Polytechnic School University of Carthage Box 743 – 2078 La Marsa, Tunisia

Abstract

The patch antenna, a key component in radio transmission channels, is appreciated for its simple construction, making it a go-to choice for receiver-transmitter systems. This research explores the use of metamaterial structures to introduce a neutralizing effect, which is advantageous in the electromagnetic field and leads to better insulation. Our proposed method aims to minimize coupling in a MIMO antenna system with antennas placed close together, at a distance of 0.5λ. We recommend a rectangular patch antenna with a full ground plane, fabricated on an RT/Duroid 5880 substrate with dimensions of $8.5\times7\times0.508$ mm^3. Simulation results show that the use of metamaterial significantly increases isolation between antennas, resulting in a notable improvement in transmission rates. To further improve network effectiveness, we propose using a linear chain composed of three Split Ring Resonators (SRR). This configuration acts as a frequency band stop filter in the range of 25.5-26.6 GHz, reducing mutual coupling between antennas in the near field and improving insulation and overall efficiencies. The implemented approach successfully reduces mutual coupling by 23 dB (for adjacent antennas) and over 10 dB (for opposite antennas) while maintaining optimal antenna performance. Therefore, our proposed antenna emerges as a strong contender for MIMO applications in the 26 GHz band, supporting 5G cellular communications.

Keywords

5G, MIMO System, SRR, Mutual Coupling 26 GHz band

1. Introduction

Given the recent progress in wireless communication technology, the fifth generation (5G) has attracted significant attention and stands out as one of the most widely discussed technologies [1]. The incorporation of millimeter-wave frequencies, specifically in the range of 24–100 GHz, for 5G applications has been made possible due to the low latency, the requirement for higher data rates, and the constrained bandwidth in the microwave spectrum range [2, 3]. Smart homes, telemedicine, virtual reality, and the Internet of Vehicles (IoV) are a few of the technologies that are anticipated to gain from the constant connectivity offered by 5G systems [4]. Governments, the telecommunications industry, and regulatory bodies are actively engaged in efforts to establish and implement 5G wireless communication networks. As per the worldwide spectrum allocation, a predominant number of countries have opted for the 26 and 28 GHz bands for 5G communication [5, 6]. Nevertheless, the design of antennas for the specific mm-Wave frequencies designated for 5G poses several challenges for antenna engineers. The demand for high-gain antennas becomes imperative in 5G communication due to atmospheric and propagation losses inherent in the mm-Wave band.

Additionally, there is very little room designated for 5G antennas in the millimeter-wave and sub-6 GHz frequency bands. The installation of many antennas in close proximity leads to strong mutual coupling and low radiation efficiency [7, 8, 9, 10, 11]. However, increasing the distance between antenna elements increases the overall volume, which is not ideal for compact devices. Therefore, reducing mutual coupling while maintaining a compact size has become a hot research topic. Only a few decoupling techniques have been reported for the millimeter-wave band [12, 13, 14, 15].

WAISS'2024: 1st Euro-Mediterranean Workshop on Artificial Intelligence and Smart Systems, October 15, 2024, Djerba, Tunisia (Co-located with the 17th International Conference on Verification and Evaluation of Computer and Communication Systems (VECoS'2024), October 15-18, 2024, Djerba, Tunisia)

*Corresponding author.

†These authors contributed equally.

linda1995chouikhi12@gmail.com (L. Chouikhi); essid.chaker@gmail.com (C. Essid); bassem.bensalah@insat.ucar.tn (B. Ben Salah)

In this study, three linear Split Ring Resonators (SRRs) are strategically positioned between adjacent or opposing antennas on the substrate layer of Rogers RT/Duroid. This placement is designed to mitigate mutual coupling arising from neighboring antenna elements, thereby ensuring effective isolation between the antennas. By accurately tuning the rejection frequency band of the SRRs, mutual coupling among components of the MIMO system can be significantly reduced, achieving insulation levels exceeding 15 dB across the frequency spectrum. Importantly, this reduction in mutual coupling is achieved without substantial alteration to the performance of the patch antenna.

2. ANTENNA DESIGNING

This section covers the suggested antenna's design and characteristics. The basic design process is illustrated in Figure 1. For 5G mm-Wave applications, the structure modeling starts with a single-element antenna measuring 8.5 × 7 mm², and then progresses to a MIMO structure made up of four similar antennas. The rectangular patch antenna is printed with the following specifications on a Rogers RT/Duroid 5880 substrate: h = 0.508 mm, $\varepsilon_r = 2.2$, and tang = 0.0009.

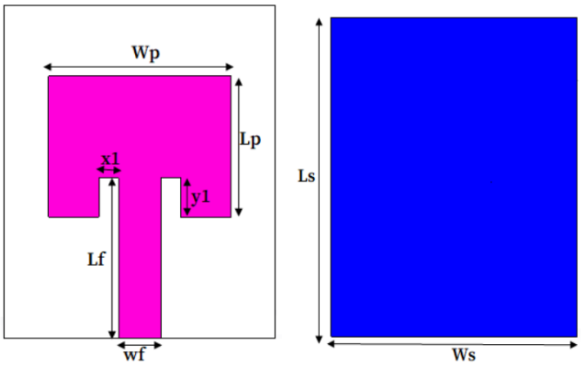

Figure 1: Design of the proposed antenna in front and bottom views.

However, the "inset feed" method is used in our research to supply or transmit electromagnetic energy to a microstrip patch antenna (the role of feeding is crucial for an antenna to operate well and to improve input impedance matching).
Using this type of microstrip line feeding technology, the feed can produce a planar structure despite the conducting strip's narrower width compared to the patch. The inset cut in the patch is designed to match the input impedance of the patch to that of the feed line without the use of any extra matching components [16]. The inset cut position and dimensions can be correctly adjusted to achieve this.
Figure 2 displays a plot of the Z-parameter to illustrate impedance matching. To match the antenna to the port, the 50 impedance must be acquired. Figure 2 clearly shows that at the resonant frequency, the imaginary component of the impedance approaches zero while the real part of the impedance is roughly 50. Consequently, the port is appropriate.

The S-parameter values S11 for the single antenna in Figure 3 show that the suggested antenna resonates in the mm-Wave frequency spectrum, between 25.5 and 26.6 GHz. According to the reflection coefficient S11 values shown in this figure, S11 is around -40 dB across the entire resonant band, has a high gain of about 7.3 dB, and has an efficiency of more than 90% (see Figures 4 and 5).

After doing a thorough parametric study, we were able to identify the parameters of our proposed antenna, which are displayed in Table 1.

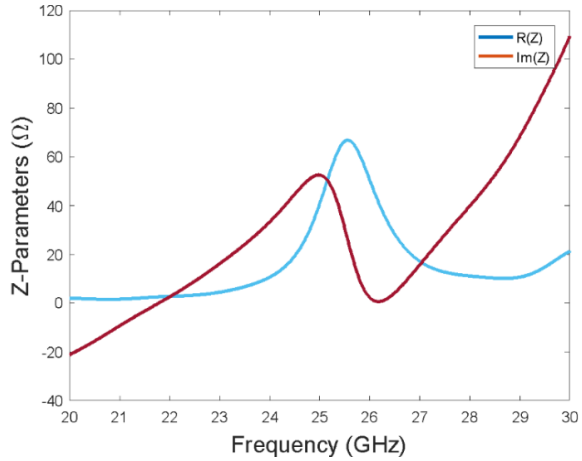

Figure 2: Curve of Z-Parameter of the studied antenna.

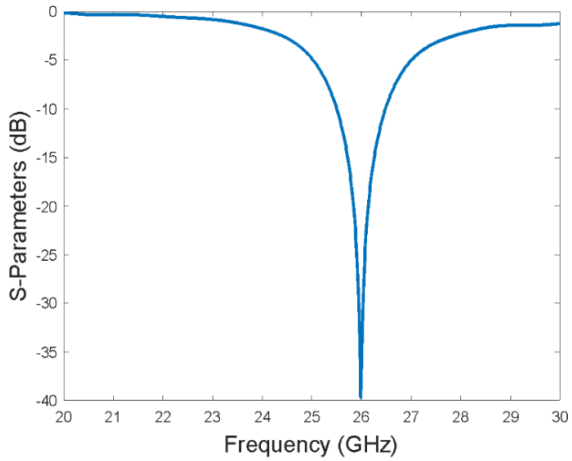

Figure 3: S-parameters of the single antenna.

Table 1
Dimensions of the proposed antenna

Parameter	Value (mm)
Ls	8.5
Ws	7
h	0.508
Lp	3.6
Wp	4.7
Wf	1.1
Lf	3.1
y1	1
x1	0.5

3. DESIGN OF MTM DECOUPLING STRUCTURES

To mitigate flux and radiation interference resulting from the close proximity of the two adjacent antennas, we propose the implementation of an electromagnetic barrier. To achieve this, we recommend the utilization of a metamaterial designed to efficiently minimize coupling rates.
Although it is well known that normal materials do not have negative dielectric constants or negative magnetic permeabilities, metamaterials can be designed in a way that satisfies both of the aforemen-

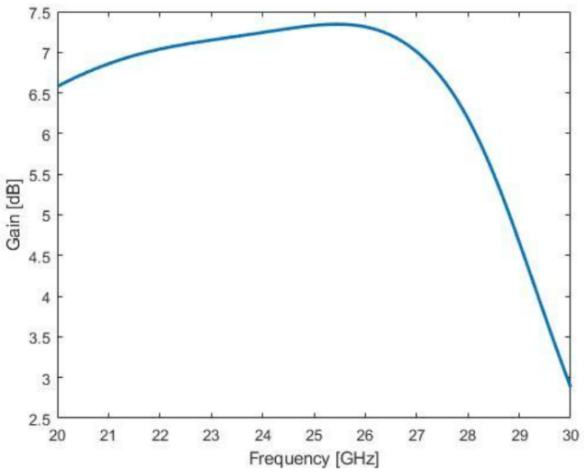

Figure 4: Gain of the proposed antenna.

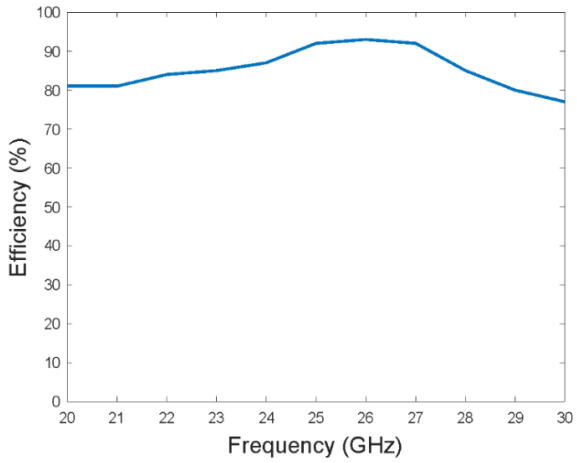

Figure 5: Efficiency of the proposed antenna.

tioned conditions while still working within the required bandwidth. We understand that the proper arrangement of a periodic cell within a metamaterial structure is all that determines how it will react. Additionally, the metamaterial structure described exhibits characteristics akin to an inductive-capacitive lumped circuit when resonances are induced within it through the inclusion of metal strips and split gaps. The design of an SRR is then modified to have an effect on the resonance of antennas that are close to one another and across from one another.
The SRR structure shown in Figure 6 will be the focus of our investigation. The SRRs' operational frequency will be 26 GHz. This resonator was constructed using PEC and was mounted on an RT/Duroid 5880 substrate (with the same characterization as the proposed antenna substrate). The exterior side of the square SRR under study is 2 mm (see Table 2).

The results of the S-parameter simulation at the resonance frequency of 26 GHz are shown in Figure 7. The SRR displays band-stop behavior close to the 26 GHz frequency. An S11 reflection has a magnitude of 0 dB with a highly attenuated S21 transmission of roughly -60 dB. This study demonstrates the existence of a band gap phenomenon close to the resonance frequency of the metamaterial cell, which is helpful for our research to minimize MC in a MIMO system. The performance of our MIMO antenna will be influenced by the design of three square SRR unit cells. Each port has a unique parameter, provided by Sij, for ports 1, 2, 3, and 4 independently and the structure of the four-component MIMO

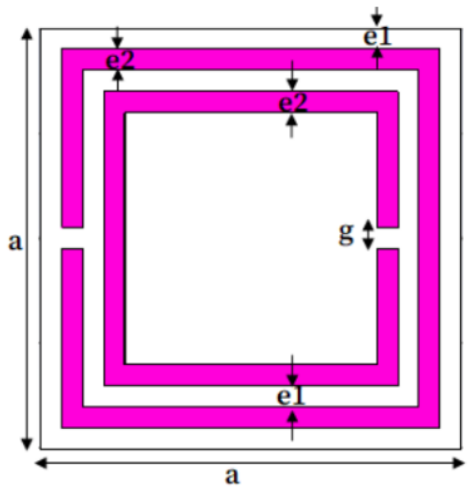

Figure 6: Structure of the SRR unit cell.

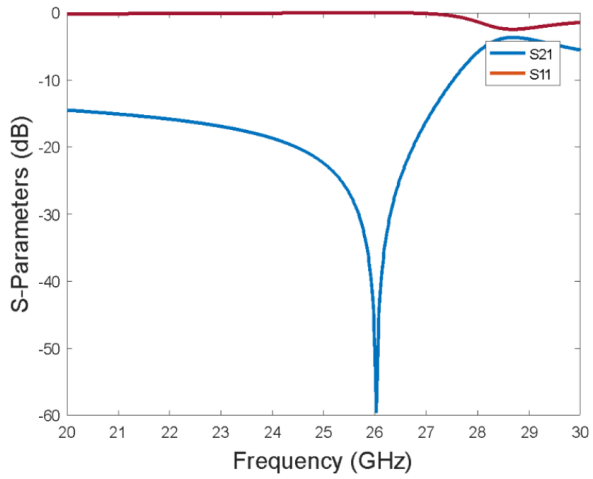

Figure 7: Simulated S-parameters of the SRR unit cell.

Table 2
SRR Dimensions.

Parameter	Value (mm)
a	2
e1	0.1
e2	0.1
g	0.1

antenna has been shown in Figures 8 and 9.
A distance of 5.73 mm (λ /2 mm) between neighbouring or opposing antennas is used, and the suggested MIMO antenna has a total size of 19.13 × 17.5 × 0.508 mm^3 with other specifications that are listed in Table 3.

The suggested MIMO antenna elements' simulated reflection coefficients (S11, S22, S33, and S44) without and with metamaterial are shown in Figures 10 and 11.

It is noteworthy, based on the depicted graphs, that the reflection coefficients of the MIMO multi-antenna system, both with and without the integration of metamaterial, are nearly identical across the entire indicated operating band. Additionally, each of these coefficients remains consistently below -10

Table 3
MIMO antennas Configurations.

Parameter	Value (mm)
L1	19.13
W1	17.5
d1	5.73
d2	5.73
d3	9.4
f1	3.5
f2	2.13

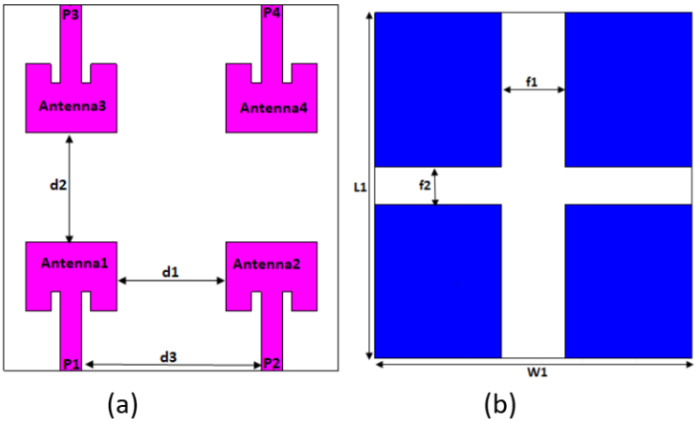

Figure 8: Structure of 4-elemnts MIMO without metamaterial: in front (a) and bottom (b) views.

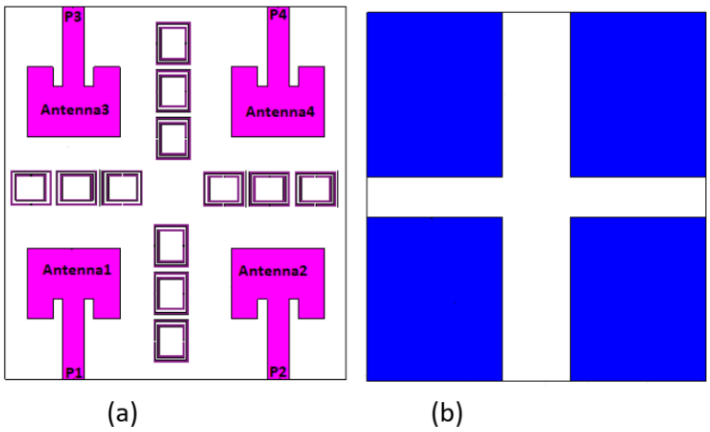

Figure 9: Structure of 4-elements MIMO with metamaterial in front (a) and bottom (b) views.

dB.

When designing a MIMO antenna, a challenging issue is electromagnetic interaction between components. Figure 12 shows how the isolation investigations show that there is less mutual coupling (S21 <-30 dB) between diagonally line antenna elements (such as between P1 and P3 or P2 and P4). However, compared to opposite antennas, the coupling between adjacent antenna elements (for example, between P1 and P2, or P3 and P4) is higher (S21 <-30 dB). This is mostly caused by the electric field's similar orientation, which raises the near field coupling. As shown by the transmission coefficient curves in Figure 13, the inclusion of SRR structures reduces the impact of near-field coupling between MIMO antennas. It should be observed that the minimum isolation increases between antenna1 and

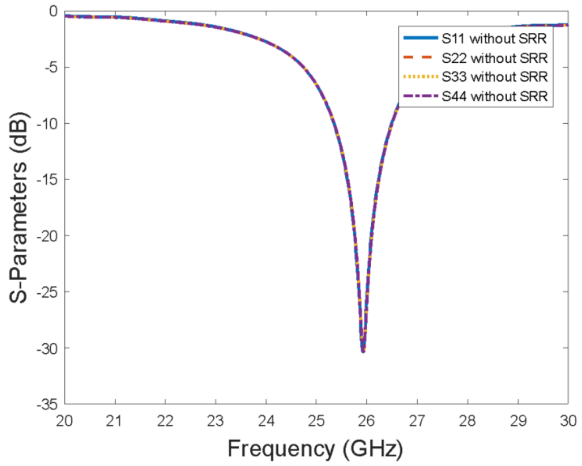

Figure 10: Return Loss of the MIMO antenna without SRR.

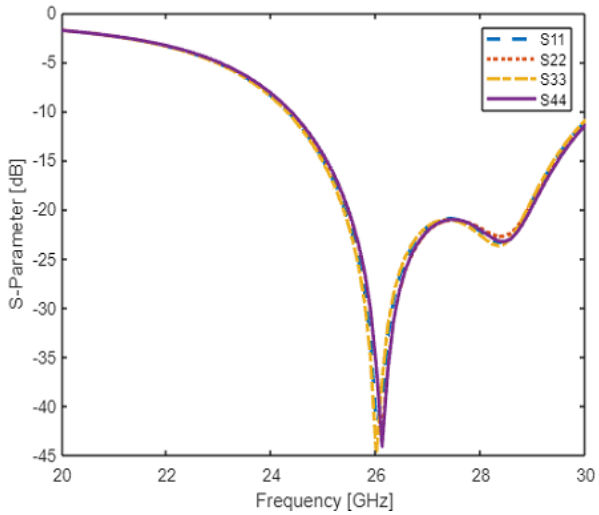

Figure 11: Return Loss of the MIMO antenna with SRR.

antenna3 (or antenna2 and antenna 4) from -21 dB to -31 dB, Meanwhile, the isolation for the remaining antenna elements surpasses this level (for example, S21<-53dB between P1 and P2 or P3 and P4).

4. CONCLUSION

This paper proposes a design for the 5G millimeter-wave frequency antenna array miniaturization. A strong isolation between the various components of our MIMO antenna is made possible by the introduction of the metamaterial between the radiating plates. The suggested antenna performs well. The application of metamaterials allowed us to successfully decouple the four side-by-side MIMO elements, employing an isolation technique tailored to this purpose. More than 20 dB less decoupling is achieved at many operating frequencies. This increases the MIMO system's transmission rate and can be applied to mobile terminals that support 26 GHz 5G mm-wave communication.

Declaration on Generative AI

The authors have not employed any Generative AI tools.

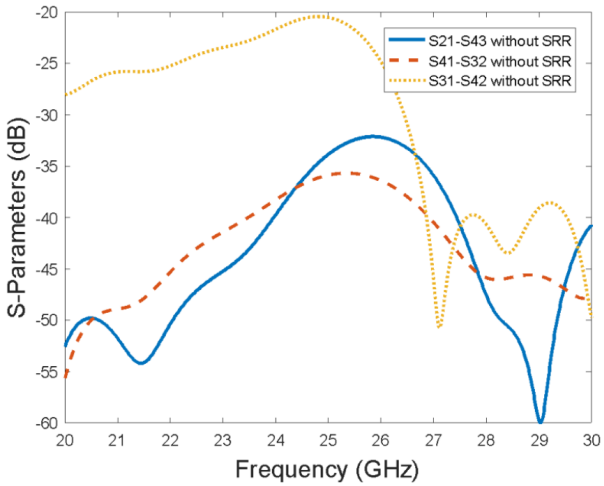

Figure 12: Transmission coefficient of the MIMO antenna without SRR.

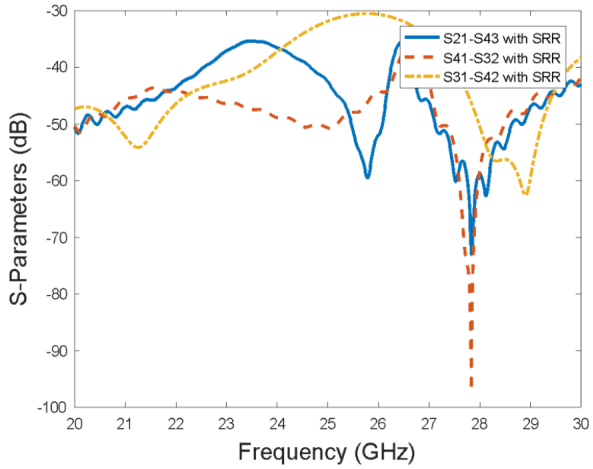

Figure 13: Transmission coefficient of the MIMO antenna with SRR.

References

[1] C. B. Sánchez, Mobile 5g millimeter-wave multi-antenna systems, Mobile Networks and Applications (2022). Preprint or report if not peer-reviewed.

[2] J. Parikh, A. Basu, Technologies assisting the paradigm shift from 4g to 5g, Wireless Personal Communications 112 (2020) 481–502.

[3] M. Shafi, A. F. Molisch, P. J. Smith, T. Haustein, P. Zhu, G. F. Pedersen, F. Tufvesson, A. Benjebbour, G. Wunder, 5g: A tutorial overview of standards, trials, challenges, deployment, and practice, IEEE Journal on Selected Areas in Communications 35 (2017) 1201–1221.

[4] M. K. Priyan, G. U. Devi, A survey on internet of vehicles: Applications, technologies, challenges and opportunities, International Journal of Advanced Intelligence Paradigms 12 (2019) 98–119.

[5] A. Hikmaturokhman, K. Ramli, M. Suryanegara, Spectrum considerations for 5g in indonesia, in: 2018 International Conference on ICT for Rural Development (IC-ICTRuDev), IEEE, 2018, pp. 1–5.

[6] A. Hikmaturokhman, K. Ramli, M. Suryanegara, Indonesian spectrum valuation of 5g mobile technology at 2600 mhz, 3500 mhz, and 26 ghz and 28 ghz, Journal of Communications 17 (2022) 294–301.

[7] H. Ullah, F. A. Tahir, A high gain and wideband narrow-beam antenna for 5g millimeter-wave applications, IEEE Access 8 (2020) 29430–29434.

[8] D. Liu, D. C. Thompson, B. Gaucher, A. J. Lalezari, W. G. Moffat, A. Natarajan, What will 5g antennas

and propagation be?, IEEE Transactions on Antennas and Propagation 65 (2017) 6205–6212.

[9] C. Abdelhamid, H. Ghariani, S. Bouallegue, A new uwb-mimo multi-antennas with high isolation for satellite communications, in: 2019 15th International Wireless Communications & Mobile Computing Conference (IWCMC), IEEE, 2019, pp. 1866–1870.

[10] C. Abdelhamid, H. Ghariani, S. Bouallegue, High isolation with metamaterial improvement in a compact uwb mimo multi-antennas, in: 2019 16th International Multi-Conference on Systems, Signals & Devices (SSD), IEEE, 2019, pp. 191–195.

[11] L. Chouikhi, C. Essid, B. B. Salah, H. Sakli, Metamaterial decoupling mimo antennas for 5g communication, in: 2021 International Conference on Software, Telecommunications and Computer Networks (SoftCOM), IEEE, 2021, pp. 1–6.

[12] M. Bilal, M. A. Imran, Q. H. Abbasi, K. D. Ahmed, S. Qaisar, S. Hussain, High-isolation mimo antenna for 5g millimeter-wave communication systems, Electronics 11 (2022) 962. doi:10.3390/electronics11060962.

[13] R. Yadav, R. D. Gupta, D. Sharma, 28 ghz inset feed circular shaped compact patch antenna array for 5g wireless communication, in: 2021 10th IEEE International Conference on Communication Systems and Network Technologies (CSNT), IEEE, 2021, pp. 17–20.

[14] Y. Ye, X. Zhao, J. Wang, Compact high-isolated mimo antenna module with chip capacitive decoupler for 5g mobile terminals, IEEE Antennas and Wireless Propagation Letters 21 (2022) 928–932. doi:10.1109/LAWP.2022.3162210.

[15] A. A. Ibrahim, M. F. A. Sree, Uwb mimo antenna with 4-element, compact size, high isolation and single band rejection for high-speed wireless networks, Wireless Networks 28 (2022) 3143–3155. doi:10.1007/s11276-021-03007-2.

[16] N. Kashyap, D. Singh, N. Sharma, Comprehensive study of microstrip patch antenna using different feeding techniques, ECS Transactions 107 (2022) 9545–9555. doi:10.1149/10701.9545ecst.